

PAPER • OPEN ACCESS

## Isotope-selective high-order interferometry with large organic molecules in free fall

To cite this article: Jonas Rodewald *et al* 2018 *New J. Phys.* **20** 033016

View the [article online](#) for updates and enhancements.

### Related content

- [Perspectives for quantum interference with biomolecules and biomolecular clusters](#)  
P Geyer, U Sezer, J Rodewald *et al.*
- [Concept of an ionizing time-domain matter-wave interferometer](#)  
Stefan Nimmrichter, Philipp Haslinger, Klaus Hornberger *et al.*
- [Experimental methods of molecular matter-wave optics](#)  
Thomas Juffmann, Hendrik Ulbricht and Markus Arndt



## PAPER

## Isotope-selective high-order interferometry with large organic molecules in free fall

## OPEN ACCESS

## RECEIVED

26 September 2017

## REVISED

9 January 2018

## ACCEPTED FOR PUBLICATION

8 February 2018



## PUBLISHED

26 March 2018

Original content from this work may be used under the terms of the [Creative Commons Attribution 3.0 licence](#).

Any further distribution of this work must maintain attribution to the author(s) and the title of the work, journal citation and DOI.



Jonas Rodewald<sup>1</sup>, Nadine Dörre<sup>1</sup>, Andrea Grimaldi<sup>1</sup>, Philipp Geyer<sup>1</sup>, Lukas Felix<sup>2</sup>, Marcel Mayor<sup>2,3,4</sup>, Armin Shayeghi<sup>1</sup>  and Markus Arndt<sup>1</sup> 

<sup>1</sup> Faculty of Physics, VCQ, University of Vienna, Boltzmannngasse 5, A-1090 Wien, Austria

<sup>2</sup> University of Basel, Department of Chemistry, St. Johannsring 1, 4056 Basel, Switzerland

<sup>3</sup> Karlsruhe Institute of Technology, Institute for Nanotechnology, D-76021 Karlsruhe, Germany

<sup>4</sup> Lehn Inst. Funct. Mat., Sun Yat-Sen University, Xin Gang Xi Rd. 135, 510275 Guangzhou, People's Republic of China

E-mail: [markus.arndt@univie.ac.at](mailto:markus.arndt@univie.ac.at)

**Keywords:** matter waves, molecular isotopes in inertial forces, quantum phenomena in gravity

### Abstract

Interferometry in the time domain has proven valuable for matter-wave based measurements. This concept has recently been generalized to cold molecular clusters using short-pulse standing light waves which realized photo-depletion gratings, arranged in a time-domain Talbot–Lau interferometer (OTIMA). Here we extend this idea further to large organic molecules and demonstrate a new scheme to scan the emerging molecular interferogram in position space. The capability of analyzing different isotopes of the same monomer under identical conditions opens perspectives for studying the interference fringe shift as a function of time in gravitational free fall. The universality of OTIMA interferometry allows one to handle a large variety of particles. In our present work, quasi-continuous laser evaporation allows transferring fragile organic molecules into the gas phase, covering more than an order of magnitude in mass between 614 amu and 6509 amu, i.e. 300% more massive than in previous OTIMA experiments. For all masses, we find about 30% fringe visibility.

### Introduction

Ever since its first conception by Louis de Broglie [1], the quantum wave nature of matter has triggered both philosophical debates and an interest in new applications. With progress in technology, atom beam splitters made of light [2, 3] and nanomechanical masks [4, 5] enabled the demonstration of advanced atom interferometers [6–8] and coherent atom optics has become a fundamental research field with intriguing opportunities in sensing of forces, fields, fundamental constants and particle properties [9, 10]. De Broglie's idea has recently been extended to cold clusters [11], plus hot [12, 13] and biological [14] molecules. For high-mass particles, it can best be tested using near-field matter-wave optics. Also in our present work, we built our experiments on the discovery by Henry F Talbot [15] that an extended optical wave can image a periodic mask without any additional optical element, simply by virtue of coherent wave propagation. Ernst Lau [16] added the insight that such lens-less imaging can even be extended to *spatially incoherent* sources, by using a first grating as a sequence of parallel slit sources to prepare spatially coherent and cylindrically expanding wavelets from any incident light field. Such array illuminators [16] have been used in light optics [17], in atom [18, 19], molecule [20] and x-ray imaging [21]—i.e. in applications where the lack of spatially coherent sources is a key challenge.

Here we implement these principles for macromolecular quantum optics, using three pulsed photo-depletion gratings to combine the idea of Talbot–Lau interferometry in position space [20, 22, 23] with that of atom optics in the time-domain [8, 24–28]. This allows realizing a molecule interferometer in the time-domain, designated as the *optical time domain matter-wave* (OTIMA) *interferometer* [11, 29]. A distinguishing element of OTIMA is the beam splitter mechanism [29, 30]: already a single vacuum ultra-violet (VUV) photon, with a wavelength of 157.6 nm, can ionize particles whose ionization potential is smaller than 7.9 eV. When such molecules encounter a VUV standing wave, they will be transmitted close to the nodes with a phase shift but

ionized and removed at the antinodes of the laser field. Three such gratings arranged in space *and* time form OTIMA, which has already been used to study the matter-wave nature of cold van der Waals clusters [11]. Measurement-induced beam splitting can also be extended to two-photon-ionization [31] or photo-fragmentation [32]. Photo-depletion gratings can address a large variety of particles in the same setting and are interesting for testing the quantum superposition principle in new complexity regimes [33] or for exploring new avenues in molecular spectroscopy [34].

Here, we study three derivatives of the organic biodye porphyrin, with different goals: tetraphenylporphyrin (1) (TPP = C<sub>44</sub>H<sub>30</sub>N<sub>4</sub>, 614 amu,  $n = 78$  atoms) is atomically defined and used for analyzing molecule interference with isotopic resolution. Its perfluoro-alkylated derivative, TPPF<sub>84</sub> (2) (C<sub>84</sub>H<sub>26</sub>F<sub>84</sub>N<sub>4</sub>S<sub>4</sub>,  $m = 2815$  amu,  $n = 202$ ) is equally well defined, more complex and yet optimized for high volatility and detectability. The most massive compound TPPF<sub>8</sub>L<sub>12</sub> (3) has been selected from a molecular library TPPF<sub>20-x</sub>L<sub>x</sub>, where  $x$  is the number of fluorinated ligands. During its synthesis, any of the 20 fluorine atoms of 5, 10, 15, 20-tetrakis (pentafluorophenyl)-21H, 23H-porphyrin may be statistically replaced by a functional chain  $L = S(CH_2)_2C_8F_{17}$ . Different molecules in the library are thus distinguished by different numbers of ligands and well-defined mass steps. We have selected TPPF<sub>8</sub>L<sub>12</sub> (3) with twelve ligands (C<sub>165</sub>H<sub>60</sub>F<sub>212</sub>N<sub>4</sub>S<sub>12</sub>), because this provided the highest signal in the experiment. The molecule contains  $n = 453$  covalently bound atoms at a mass around 6509 amu. Even for the same chemical sum formula, the library still contains a variety of structural isomers, differing in constitution and conformation. All members of one mass in the family are expected to be very similar in their electrical and optical properties, since all side-chains are identical and electronically only weakly coupled to the porphyrin core which dominates the molecular UV/VIS response and their susceptibility to VUV photoionization [35]. Compounds (1) and (3) differ by an order of magnitude in mass.

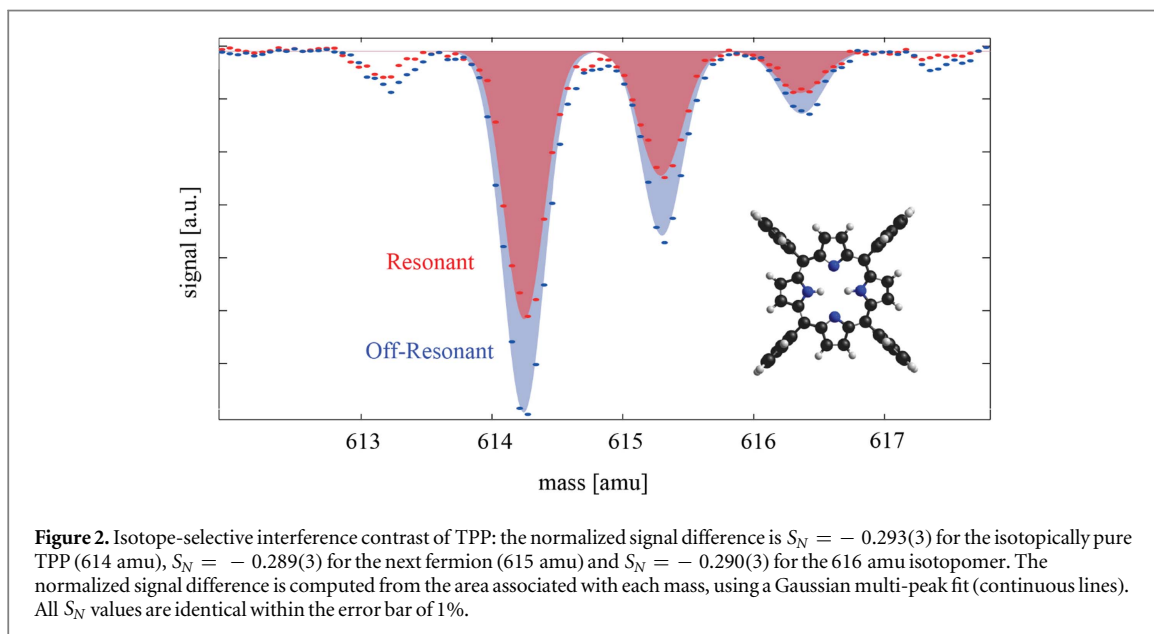
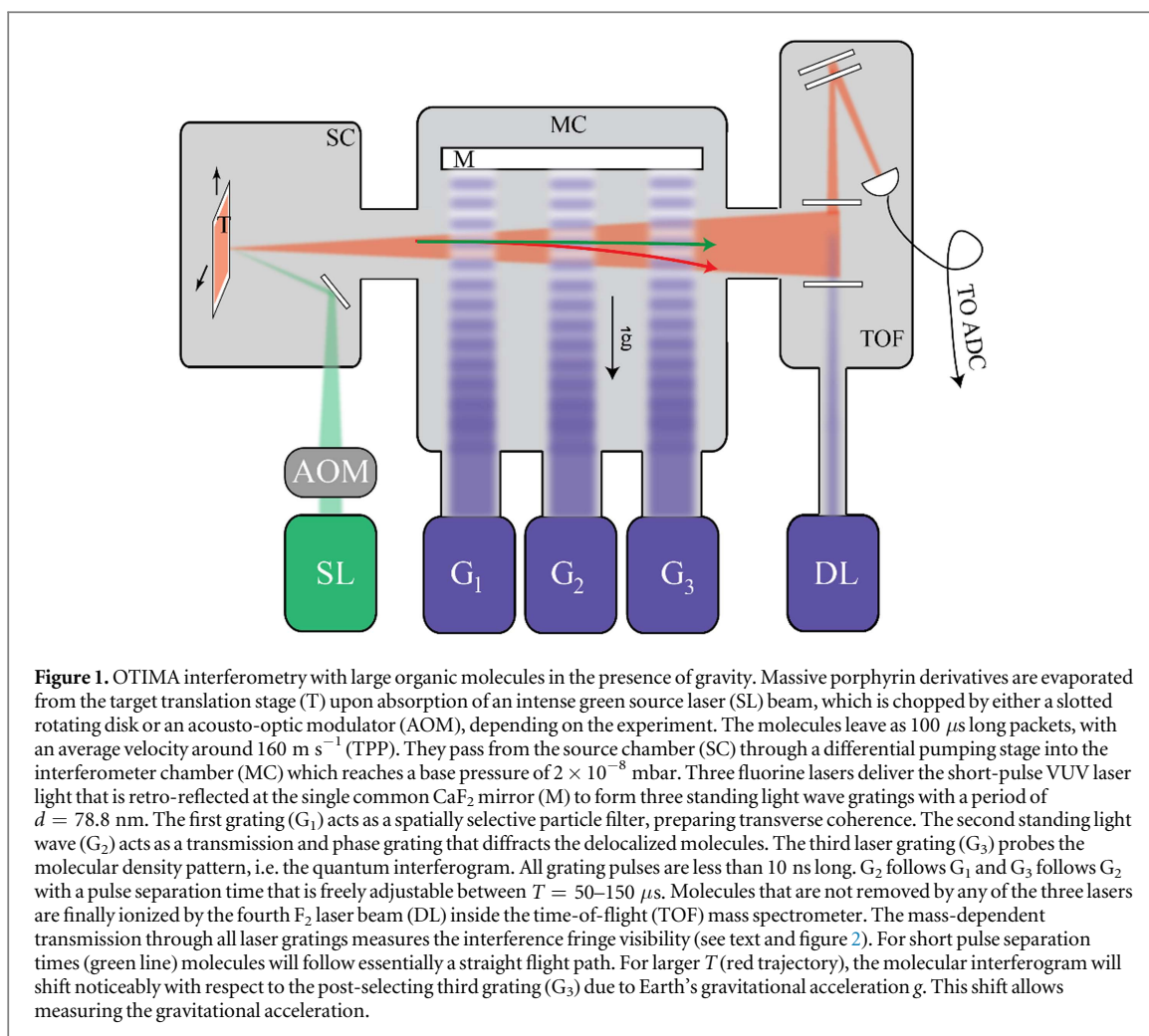
We launch the porphyrins and their large derivatives using long-pulse laser evaporation which provides three times slower forward velocities compared to typical supersonic beams [11]. This enables studies that had remained inaccessible before: firstly, the gravitational fringe shift is an order of magnitude larger than in earlier experiments, and becomes measurable in OTIMA interferometry since the interference fringe shift depends quadratically on the transit time and thus on the velocity like  $1/v^2$ . Secondly, the low velocities allow studies with 6509 amu particles, which is a mass record for the OTIMA interferometer. Only one other experiment so far, the Vienna Kapitza–Dirac–Talbot–Lau interferometer [13, 23] has been capable of exploring this mass scale. Here we probe that mass range using an entirely independent setup, based on a novel source technique, working with photodepletion beam splitters, operating in the time-domain and profiting from a different detection scheme with better mass and time resolution. OTIMA thus provides an important independent corroboration of the quantum wave nature of hot and large organic molecules that are more massive even than a small protein such as insulin.

## Experimental setup

We coat molecules with a layer thickness of ca. 10  $\mu\text{m}$  onto a 50  $\times$  50 mm<sup>2</sup> glass plate, which is mounted to a 2D-translation stage (see figure 1). Molecular sublimation is induced by a 5 Watt green (532 nm) diode-pumped solid state laser beam (Coherent Verdi), focused onto the sample plate with a beam waist of ca. 100  $\mu\text{m}$ . To ensure that all molecules interact with the same grating pulse sequence, the green beam is chopped into pulses of less than 100  $\mu\text{s}$  duration and 500  $\mu\text{J}$  energy, with a repetition rate of 100 Hz. Pulsed laser heating is local and short. It is softer than evaporation in an oven and is well compatible with time-of-flight (TOF) velocity selection, which is required for OTIMA. On the other hand, evaporation in 100  $\mu\text{s}$  long pulses delivers a substantially higher molecular flux than matrix assisted laser desorption (MALD) which operates with nanosecond pulses [36]. A pulse duration of 100  $\mu\text{s}$  was the best compromise between high signal, low velocity and low thermal damage and was crucial for launching sizable pulses of isolated TPPF<sub>8</sub>L<sub>12</sub> molecules.

We find a mean forward velocity of  $v = 160 \text{ m s}^{-1}$  for TPP (614 amu) with a FWHM spread of  $75 \text{ m s}^{-1}$ . This is similar to the  $160 \text{ m s}^{-1}$  observed with nine times more massive TPPF<sub>8</sub>L<sub>12</sub> molecules (6509 amu). For TPPF<sub>84</sub> we employed a MALD technique, using a short-pulse optical parametric oscillator (EKSPLA OPO) with a wavelength of  $\lambda = 640 \text{ nm}$ , a pulse energy of 3 mJ in 100  $\mu\text{m}$  focal diameter, 7 ns pulse duration and a repetition rate of 100 Hz. This generated a much higher velocity of  $350 \text{ m s}^{-1}$ . If we were to interpret these beams as thermal, we would derive molecular temperatures of 1000 K (TPP), 20 000 K (TPPF<sub>8</sub>L<sub>12</sub>) and 8500 K (TPPF<sub>84</sub>), respectively.

A TPP temperature of 1000 K is still consistent with the observation that all molecules stay intact except for the possible loss of one or two Hydrogen atoms during launch (see figure 2). However, we need to invoke a different mechanism, to explain the behavior of the functionalized porphyrins. The results resemble self-seeded MALD, where some of the functionalized porphyrins eject one or more ligand chains [37]. This ligand gas can



entrain intact members of the functionalized porphyrin library. A ligand gas temperature of  $1000 \text{ K}$  is consistent with the observed velocities for both  $\text{TPPF}_8\text{L}_{12}$  and  $\text{TPPF}_8\text{L}_{84}$ .

The molecular beam is collimated to a width and height of  $600 \times 1000 \mu\text{m}^2$  right before the first grating. Three fluorine lasers (GAM EX50) emit VUV pulses, each with a duration of  $\tau = 10 \text{ ns}$ , a pulse energy of  $E_p = 3 \text{ mJ}$  and a repetition rate of  $100 \text{ Hz}$ . Their flat top beam profiles of  $1 \times 10 \text{ mm}^2$  are oriented with the

longer axis parallel to the molecular beam. All laser beams are retro-reflected at the same super-polished CaF<sub>2</sub> mirror and every such standing light-wave acts as a single-photon ionization mask with a period of  $d = 78.8$  nm. For compounds (2) and (3) competing two-photon or fragmentation processes in the grating antinodes cannot be excluded. However, earlier experiments have showed that dissociation-induced recoil would deflect the molecules beyond the detector acceptance angle [32]. Molecular beam depletion in the optical grating thus mimics a free-standing material structure and imprints a nanoscale density pattern onto the molecular beam. Three such gratings, G<sub>1</sub>, G<sub>2</sub> and G<sub>3</sub>, arranged in space and time form a matter-wave interferometer, where the wave function of every individual particle is coherently split in G<sub>1</sub>, diffracted and redirected at G<sub>2</sub> and recombined at G<sub>3</sub>.

A small effective slit width in G<sub>1</sub> prepares a large momentum uncertainty of the transmitted molecules and thus creates transverse coherence in the molecular beam further downstream. It is required to illuminate each pair of neighboring nodes in G<sub>2</sub> with a fixed de Broglie wave phase. The coherent evolution of the molecular matter-wave further leads to lens-less self-imaging of G<sub>2</sub> and the emergence of a molecular density pattern. This pattern appears within a time window of several nanoseconds and at a location behind G<sub>2</sub> that is determined by the molecular mass and velocity.

All three gratings additionally imprint position-dependent phases onto the matter-wave. This arises because of the dipole interaction between the electric field gradients in the standing wave and the optical polarizability of the molecule. It influences all molecules in G<sub>2</sub>. In G<sub>1</sub>, these additional phase shifts play no role since the molecules arrive with arbitrary phases from the incoherent thermal source. Phase shifts in G<sub>3</sub> do not matter since the detector following the third grating spatially integrates over the molecular density pattern. If all three grating vectors are parallel and of equal length, the relative phase between the interference pattern and G<sub>3</sub> will modulate the number of molecules transmitted through G<sub>3</sub>. A fourth F<sub>2</sub> laser (Coherent Excistar XS,  $\tau = 5$  ns,  $E_p = 1.5$  mJ,  $\lambda_L = 157.6$  nm), a few centimetres further downstream, ionizes these molecules, which are then mass-analyzed and counted by the TOF mass spectrometer.

Molecules arriving with different velocities contribute to interference patterns at different locations. In time-domain interferometry one copes with that by exposing all molecules at the same time to the same laser field, independent of their location and velocity. A high-contrast molecular density pattern forms—when the separation between two subsequent laser grating pulses  $\Delta T$  is close to a multiple  $n$  of the Talbot time [29]  $T_T = md^2/h$ , where  $h$  is Planck's constant. The interference contrast or fringe visibility is highest when the two pulse-separation times  $\Delta T_{12}$  and  $\Delta T_{23}$  between subsequent grating pairs are equal. If the difference between the pulse separation times  $\delta T = |\Delta T_{12} - \Delta T_{23}|$  exceeds several 10 ns, the interference contrast vanishes.

We toggle the experiment between a symmetric, (*resonant*,  $\delta T \leq 1$  ns) and an asymmetric (*off-resonant*  $\delta T \geq 200$  ns) mode and record the full mass spectrum transmitted behind G<sub>3</sub> in both situations, designated as  $S_{\text{res}}$  and  $S_{\text{off}}$ . For every mass peak one can define the normalized signal difference  $S_N = (S_{\text{res}} - S_{\text{off}})/S_{\text{off}}$  as a measure of the interference fringe visibility [11].

## Results and discussion

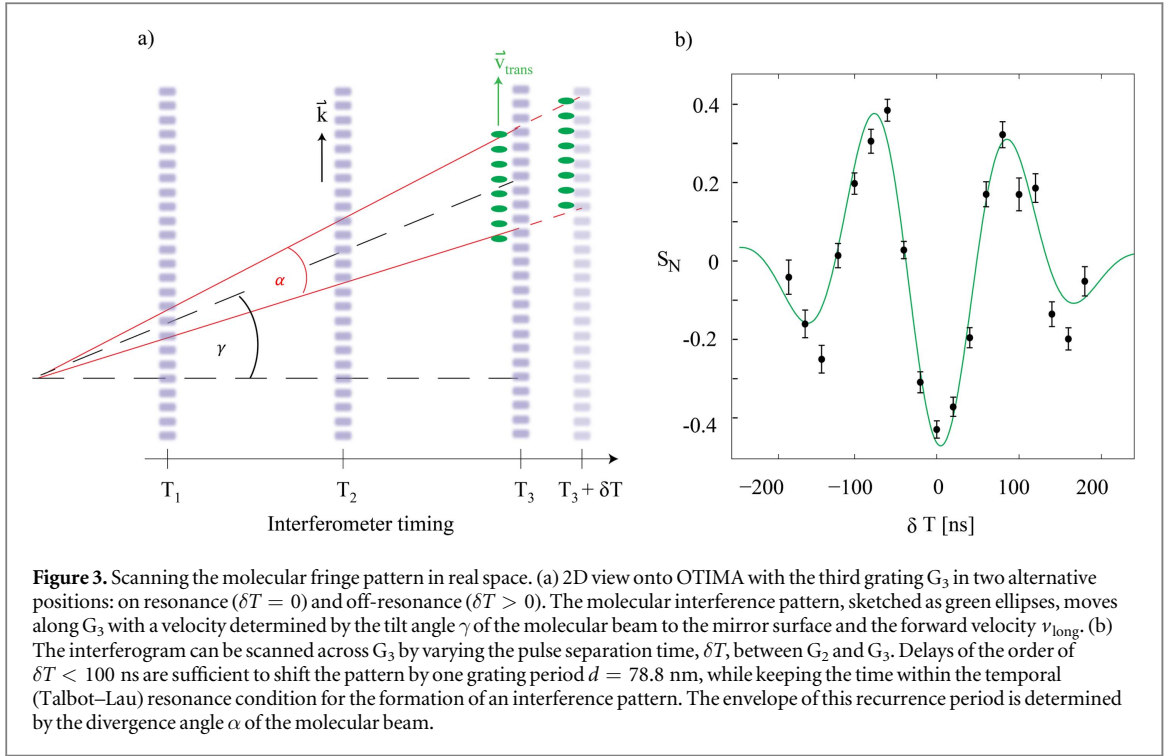
### Isotope-selective interference of TPP

Figure 2 displays a typical TPP mass spectrum for *resonant* (red dots,  $\delta T = 0$  ns) and *non-resonant* (blue dots,  $\delta T = 200$  ns) pulse separation times. The peak at 614.25 amu corresponds to the isotopically pure porphyrin molecule, for which we find an interference contrast of  $S_N = 29 \pm 1\%$  for a pulse separation time of  $\Delta T = 104$   $\mu$ s. This is within the 11th Talbot resonance, with a nominal Talbot time of  $T_T = 9.558$   $\mu$ s. Since the fermionic isotope <sup>13</sup>C occurs with a natural abundance of 1%, more than 61.1% of all molecules are isotopically pure, 30.3% contain a single <sup>13</sup>C isotope, 7.3% exactly two of them and 1.1% three such nuclei. An unexpected small mass peak, 1 amu (very rarely even 2 amu) below the isotopically pure TPP, is attributed to the thermal loss of one hydrogen atom during the heating process. If this occurs, every mass peak is contaminated by a small percentage of the next higher isotopomer.

Even though theory [29] allows contrast values as high as 100%, the finite laser power, the non-unity mirror reflectivity and mirror corrugations on the level of  $\pm 5$  nm limit the maximal contrast [38]. Vibrational dephasing [39], thermal [40] or collisional [41, 42] decoherence do not constrain the visibility. We find about the same interference contrast for masses varying by as much as a factor of ten and transit times by a factor of three, as long as the VUV standing light wave grating power is set to achieve the same overall particle transmission of less than 30% (see below).

### A time-domain tool to probe the interferogram in position space

In many contrast interferometers [9, 43], one can visualize interference by scanning the third grating across the interferogram. In OTIMA, this is difficult because all lasers are reflected by the same fixed mirror. Here, we



reverse the strategy and ask how to scan the molecular pattern across  $G_3$  rather than  $G_3$  over the molecular beam. The TPP particle beam was collimated to an angle  $\alpha$  and aligned under the tilt angle  $\gamma$  to the mirror surface, as depicted in figure 3. This way the molecular fringe pattern at  $G_3$  acquires a velocity component  $v_{\text{trans}} = \gamma v$  normal to the mirror and therefore runs along  $G_3$ . Delaying the laser pulse in  $G_3$  by  $\delta T = \pm \delta T_{\text{coh}} = d/(2v_{\text{trans}})$ , one can thus map the real space molecular fringe pattern. At larger delays, the coherent wave evolution reduces the fringe contrast again.

We demonstrate this phenomenon in figure 3(b), by plotting the normalized signal difference  $S_N$  as function of  $\delta T$ , for a pulse separation time  $\Delta T = 75.1 \mu\text{s}$ , close to the 8th order Talbot resonance for TPP. We fit equation (1) to the data, to extract the fringe period  $\sigma$  and the width of the resonance dip:

$$S_N(\delta T) = V_0 \exp \left[ - \left( \frac{\delta T}{\sigma_T \sqrt{2}} \right)^2 \right] \cos \left( 2\pi \frac{\delta T - \delta T_{\text{off}}}{\sigma} \right), \quad (1)$$

where the overall visibility  $V_0$  and the offset time  $\delta T_{\text{off}}$  are experimental fit parameters. The width  $\sigma_T$  of the symmetric Gaussian resonance curve at  $1/10$  of the maximum is related to the divergence  $\alpha$  and yields

$$\alpha = \arcsin \left( \frac{d}{2\sigma_T v_{\text{long}} \sqrt{2 \ln(10)}} \right) = 0.9 \pm 0.2 \text{ mrad}. \quad (2)$$

The period  $\sigma$  of the pattern is related to the molecular beam inclination

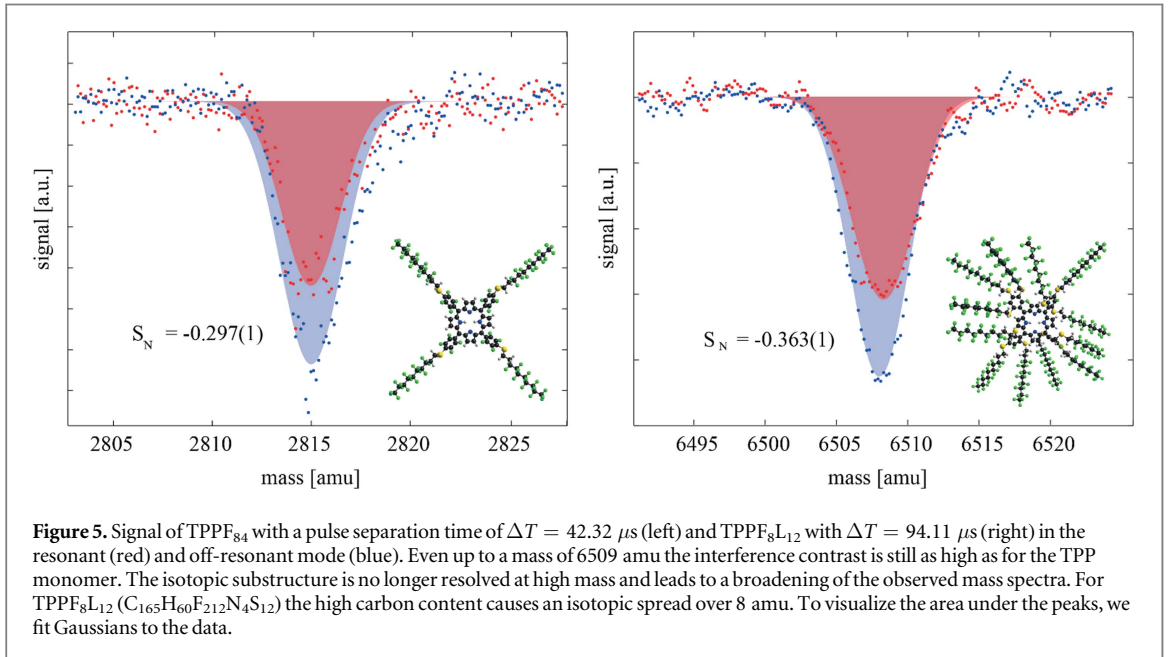
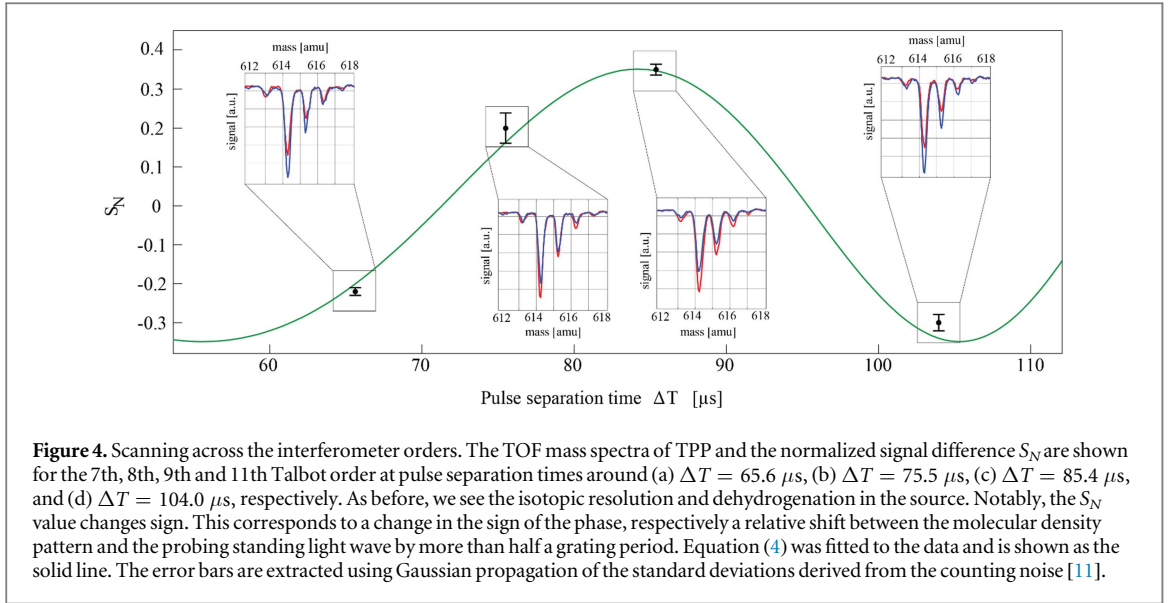
$$\gamma = \arcsin \left( \frac{d}{\sigma v_{\text{long}}} \right) = 2.4 \pm 0.1 \text{ mrad}, \quad (3)$$

in good agreement with the experimental beam parameters. The time dependence of the normalized signal difference thus provides clear evidence for the formation of a molecular density pattern with a period of  $d = 78.8$  nm in equation (1).

### Isotope-selective high-order interference in gravitational free fall

To probe the free fall of molecules, we use the fact that the pulse separation times vary by almost a factor of two between the 7th, 8th, 9th and 11th Talbot order. The resulting TPP mass spectra and contrast values are shown as insets in figures 4(a)–(d). The fine structure in the mass spectrum shows that we can monitor 3–4 different isotopes of the same molecule under identical conditions. For our subsequent high-mass experiments it is also important to note that the fringes of the highest order show the same contrast as the lower ones. This indicates that acoustic dephasing, collisional and thermal decoherence are still negligible on these time scales.

Varying the pulse separation time by a factor of two changes the free fall distance by a factor of four. This is sufficient for the interferogram at  $G_3$  to fall alongside two grating periods. We illustrate this in figure 4, noting



that the negative sign of the fringe contrast corresponds to a shift of the fringe pattern by half a grating period. The data of figure 4 can be fit by equation (4) using the gravitational acceleration  $g = 9.81 \text{ m s}^{-2}$ , the pulse separation time  $\Delta T$  and the observed contrast:

$$S_N(\Delta T) = V_0 \sin \left[ \frac{2\pi}{d} (b - g(\Delta T)^2) \right]. \quad (4)$$

We find a sine fringe contrast of  $V_0 = 34.4 \pm 0.5\%$  and a vertical offset  $b = 10 \text{ nm}$ , the latter being consistent with local mirror deformations [38] and without further significance as long as it remains stable. Since the optical gratings cannot be moved in space, the range of accessible symmetric pulse separation times is currently limited to the width of the detected velocity distribution. We assume that the optical molecular properties do not change as a function of their velocity. While this assumption would not need any explanation for atoms—except for the obvious small Doppler shifts—experiments with nanosecond laser desorption have seen a correlation between internal temperature and kinetic energy [35]. However, in a quasi-thermal long-pulse process as used here, the internal temperature, which defines the spectrum, is expected to be equilibrated and independent of velocity.

### High-mass interference

OTIMA can cover a large mass range in the same setting. We demonstrate this in figure 5 for the organic macromolecules TPPF<sub>84</sub> and TPPF<sub>8L12</sub>, where the normalized signal difference  $S_N(m)$  measures again the fringe visibility. We determine the signal in the resonant ( $S_{\text{res}}$ ) and off-resonant mode ( $S_{\text{off}}$ ) by integrating over the relevant peaks in the mass spectra and arrive at  $S_N$  via  $S_N = (S_{\text{res}} - S_{\text{off}}) / S_{\text{off}}$ . The contrast and its resonance structure in the time domain are consistent with the expectations for a quantum revival of the molecular density pattern caused by the Talbot–Lau effect. A detailed quantitative comparison hinges on the optical polarizability and absolute absorption cross section in the vacuum ultraviolet range (157 nm), for which independent literature data are unavailable. In all three cases, TPP, TPPF<sub>84</sub> and TPPF<sub>8L12</sub> the laser intensities were chosen such as to ensure a beam depletion in the standing light wave of 30%. The effective grating opening is therefore comparable in all three cases and the experiment shows that also the resulting interference contrast always achieves about 30% or more. Note that, even if the fringe pattern could additionally be explained by a classical Moiré effect, for very short de Broglie wavelengths and certain fringe contrast values, it would still perfectly serve to characterize the molecular response in gravity or electro-magnetic fields.

### Conclusion

OTIMA differs from atom interferometers with optical gratings, which are typically optimized for at most two atomic species or isotopes. Photodepletion gratings enable the coherent manipulation of particles that may cover an order of magnitude in mass, already now, and even more in the future. Figures 4 and 5 thus suggest the possibility of exploring gravitational free fall, for a large variety of complex quantum particles, fermions or bosons, low and high mass, organics, metals or semiconductors, in the same machine, using similar sources, the same gratings and the same detector.

In our proof-of-principle demonstration in figure 2, we measure the same normalized signal difference  $S_N$  for all TPP isotopomers to within an uncertainty  $\Delta S_N = 0.01$ . This translates into an uncertainty in the gravitational acceleration  $\Delta g$  of

$$\Delta g = -\frac{d}{2\pi(\Delta T)^2} \cdot \frac{\Delta S_N}{\sqrt{V_0^2 - S_N^2}} \quad (5)$$

and a relative uncertainty of better than 1% in less than an hour of measurement. Modern tests of the equivalence principle with atoms have measured [44, 45] Eötvös parameters better than  $\eta \leq (g_2 - g_1) / g_1 \leq 10^{-8} - 10^{-7}$  when comparing the gravitational acceleration  $g_1$  and  $g_2$  of two different alkalis [45], two isotopes or hyperfine states [46] or Zeeman states of the same atom [47]. Atomic fountain experiments [48] may soon approach  $\eta = 10^{-13}$ . Reaching such accuracy levels with large molecules will require substantial improvements in the preparation of cold beams of macromolecules with high phase space density. Our present Eötvös value is comparable with the historically first gravity experiments in neutron interference [49] as well as with recent proposals for free-falling anti-hydrogen [50]. New systems may address questions that have not been asked in a previous context so far. It has been proposed for example that the isospin ratio of two test particles might be an important criterion in tests of the equivalence principle [51]. In our present experiments, the isospin-to-mass-ratio changes by only 0.16% between neighboring isotopomers. However, interferometry with large molecules allows the comparing of the freefall of particles with vastly different masses or conformations with different internal excitation energies, binding energies, different spins, different angular momenta, comparing localized or delocalized electrons and therefore different magnetic moments or even different chiralities. Our work outlines the potential of future experiments and aims at stimulating the discussion about the relevance of internal particle properties that have rarely been considered in previous models so far.

### Competing financial interests

The authors declare no competing financial interests.

### Acknowledgments

This work has received funding from the European Research Council (ERC) under the European Union's Horizon 2020 research and innovation programme (grant agreement no. 320694), the Austrian Science Funds FWF W1210-N25, the Swiss National Science Foundation (200020\_159730), and the Swiss Nanoscience Institute (P1403). We acknowledge association with the research platform TURIS at the University of Vienna and very fruitful discussions with Philipp Haslinger.



## ORCID iDs

Armin Shayeghi  <https://orcid.org/0000-0003-3154-1195>

Markus Arndt  <https://orcid.org/0000-0002-9487-4985>

## References

- [1] Broglie L D 1923 *Nature* **112** 540–540
- [2] Moskowitz P E, Gould P L, Atlas S R and Pritchard D E 1983 *Phys. Rev. Lett.* **51** 370–3
- [3] Gould P L, Ruff G A and Pritchard D E 1986 *Phys. Rev. Lett.* **56** 827–30
- [4] Keith D W, Schattenburg M L, Smith H I and Pritchard D E 1988 *Phys. Rev. Lett.* **61** 1580–3
- [5] Carnal O and Mlynek J 1991 *Phys. Rev. Lett.* **66** 2689–92
- [6] Bordé C J 1989 *Phys. Lett. A* **140** 10–2
- [7] Keith D W, Ekstrom C R, Turchette Q A and Pritchard D E 1991 *Phys. Rev. Lett.* **66** 2693
- [8] Kasevich M and Chu S 1991 *Phys. Rev. Lett.* **67** 181–4
- [9] Cronin A D, Schmiedmayer J and Pritchard D E 2009 *Rev. Mod. Phys.* **81** 1051–129
- [10] Tino G and Kasevich M 2014 *Atom Interferometry* (Amsterdam: IOS Press)
- [11] Haslinger P, Dörre N, Geyer P, Rodewald J, Nimmrichter S and Arndt M 2013 *Nat. Phys.* **9** 144–8
- [12] Juffmann T, Ulbricht H and Arndt M 2013 *Rep. Prog. Phys.* **76** 086402
- [13] Eibenberger S, Gerlich S, Arndt M, Mayor M and Tüxen J 2013 *Phys. Chem. Chem. Phys.* **15** 14696–700
- [14] Mairhofer L, Eibenberger S, Cotter J P, Romirer M, Shayeghi A and Arndt M 2017 *Angew. Chem. Int. Ed. (online pub)* **56** 10947–51
- [15] Talbot W H F 1836 *Phil. Mag.* **9** 401–7
- [16] Lau E 1948 *Ann. Phys.* **6** 417
- [17] Paturski K 1989 *Progress in Optics* vol XXVII ed E Wolf (Amsterdam: Elsevier) pp 2–108
- [18] Clauser J F and Li S 1994 *Phys. Rev. A* **49** R2213
- [19] Chapman M S, Ekstrom C R, Hammond T D, Schmiedmayer J, Tannian B E, Wehinger S and Pritchard D E 1995 *Phys. Rev. A* **51** R14
- [20] Brezger B, Hackermüller L, Utenthaler S, Petschinka J, Arndt M and Zeilinger A 2002 *Phys. Rev. Lett.* **88** 100404
- [21] Pfeiffer F, Bech M, Bunk O, Kraft P, Eikenberry E F, Bronnimann C, Grunzweig C and David C 2008 *Nat. Mater.* **7** 134–7
- [22] Brezger B, Arndt M and Zeilinger A 2003 *J. Opt. B* **5** 82–9
- [23] Gerlich S et al 2007 *Nat. Phys.* **3** 711–5
- [24] Cahn S B, Kumarakrishnan A, Shim U, Sleator T, Berman P R and Dubetsky B 1997 *Phys. Rev. Lett.* **79** 784–7
- [25] Szriftgiser P, Guéry-Odelin D, Arndt M and Dalibard J 1996 *Phys. Rev. Lett.* **77** 4–7
- [26] Bernet S, Abfalterer R, Keller C, Schmiedmayer J and Zeilinger A 1998 *J. Opt. Soc. Am. B* **15** 2817–22
- [27] Hinderthur H, Ruschewitz F, Lohe H J, Lechte S, Sengstock K and Ertmer W 1999 *Phys. Rev. A* **59** 2216–9
- [28] Deng L, Hagley E W, Denschlag J, Simsarian J E, Edwards M, Clark C W, Helmerson K, Rolston S L and Phillips W D 1999 *Phys. Rev. Lett.* **83** 5407–11
- [29] Nimmrichter S, Haslinger P, Hornberger K and Arndt M 2011 *New J. Phys.* **13** 075002
- [30] Reiger E, Hackermüller L, Berninger M and Arndt M 2006 *Opt. Commun.* **264** 326–32
- [31] Walter K, Nimmrichter S and Hornberger K 2016 *Phys. Rev. A* **94** 043637
- [32] Dörre N, Rodewald J, Geyer P, von Issendorff B, Haslinger P and Arndt M 2014 *Phys. Rev. Lett.* **113** 233001
- [33] Nimmrichter S, Hornberger K, Haslinger P and Arndt M 2011 *Phys. Rev. A* **83** 043621
- [34] Rodewald J, Haslinger P, Dörre N, Stickler B A, Shayeghi A, Hornberger K and Arndt M 2016 *Appl. Phys. B* **123** 3
- [35] Schmid P, Stöhr F, Arndt M, Tüxen J and Mayor M 2013 *J. Am. Soc. Mass Spectrom.* **24** 602–8
- [36] Karas M, Bachmann D, Bahr U and Hillenkamp F 1987 *Int. J. Mass Spectrom. Ion Process.* **78** 53
- [37] Gallego A, Sezer U, Arndt M and Mayor M 2017 *Nanoscale* **9** 9175–80
- [38] Dörre N, Haslinger P, Rodewald J, Geyer P and Arndt M 2015 *J. Opt. Soc. Am. B* **32** 114
- [39] Stibor A, Hornberger K, Hackermüller L, Zeilinger A and Arndt M 2005 *Laser Phys.* **15** 10–7
- [40] Hackermüller L, Hornberger K, Brezger B, Zeilinger A and Arndt M 2004 *Nature* **427** 711–4
- [41] Hornberger K and Sipe J E 2003 *Phys. Rev. A* **68** 12105
- [42] Hornberger K, Sipe J E and Arndt M 2004 *Phys. Rev. A* **70** 53608
- [43] Hornberger K, Gerlich S, Haslinger P, Nimmrichter S and Arndt M 2012 *Rev. Mod. Phys.* **84** 157–73
- [44] Barrett B, Antoni-Micollier L, Chichet L, Battelier B, Gominet P A, Bertoldi A, Bouyer P and Landragin A 2015 *New J. Phys.* **17** 085010
- [45] Schlippert D, Hartwig J, Albers H, Richardson L L, Schubert C, Roura A, Schleich W P, Ertmer W and Rasel E M 2014 *Phys. Rev. Lett.* **112** 203002
- [46] Fray S, Diez C A, Hänsch T W and Weitz M 2004 *Phys. Rev. Lett.* **93** 240404
- [47] Duan X-C, Deng X-B, Zhou M-K, Zhang K, Xu W-J, Xiong F, Xu Y-Y, Shao C-G, Luo J and Hu Z-K 2016 *Phys. Rev. Lett.* **117** 023001
- [48] Asenbaum P, Kovachy T, Brown D D, Hogan J M and Kasevich M A 2017 *Phys. Rev. Lett.* **118** 183602
- [49] Collela R, Oberhauser A W and Werner S A 1975 *Phys. Rev. Lett.* **34** 1472–4
- [50] Aghion S et al 2013 *J. Instrum.* **8** P08013–08013
- [51] Hohensee M A and Müller H 2011 *J. Mod. Opt.* **58** 2021–7